Utah State University

DigitalCommons@USU

Space Dynamics Laboratory Publications

Space Dynamics Laboratory

1-1-1988

Comparison of Simultaneous MST Radar and Electron Density Probe Measurements During STATE

J. C. Ulwick

K. D. Baker

M. C. Kelley

B. B. Balsley

W. L. Ecklund

Follow this and additional works at: https://digitalcommons.usu.edu/sdl_pubs

Utah State University
MERRILL-CAZIER LIBRARY

Comparison of Simultaneous MST Radar and Electron Density Probe Measurements During STATE

J. C. Ulwick and K. D. Baker

Department of Electrical Engineering, Utah State University, Logan

M. C. Kelley

School of Electrical Engineering, Cornell University, Ithaca, New York

B. B. Balsley and W. L. Ecklund

Aeronomy Laboratory, National Oceanic and Atmospheric Administration, Boulder, Colorado

During the Structure and Atmospheric Turbulence Environment (STATE) campaign in June 1983, three small rockets (Super Arcas) containing dc probes to measure electron density irregularities with high spatial resolution were launched at Poker Flat, Alaska. The rockets were launched at three different times when the nearby MST (mesospheric, stratospheric, and tropospheric) radar showed intense regions of backscatter in the mesosphere. The first and third flights (STATE 1 and STATE 3) were perfectly successful, providing high-quality electron density measurements; STATE 2 did not produce any useful results. When the electron density measurements are compared with the radar echo power as a function of altitude for STATE 1 and 3, large fluctuations and strong gradients in the electron density profiles are observed in the region of most intense backscatter. The electron density profiles show different characteristics in the peak scattering region with respect to altitude, electron density gradients, and irregularities. Power spectra of the electron density spatial fluctuations were derived from the measured electron densities for the region from approximately 65 to 90 km for several height intervals, with the smallest being approximately 100 m. In the region of most intense backscatter, the spectral power over the entire frequency range increases by almost 3 orders of magnitude for both rocket data sets. For STATE 1 a linear fit to the log-log power spectral plots between 1.0–80 Hz (i.e., spatial scales from about 500 to 5 m) can be approximated by a power law with an index of about −(5/3), as would be expected in an inertial subrange of homogeneous, isotropic turbulence. The spectra, moreover, show a continuous steepening of the spectral slope in the viscous subrange at frequencies above 100 Hz (approximately 4.5–0.5 m), giving a much higher spectral index. The STATE 3 spectra, on the other hand, show a steeper spectral index near −2.0 in the inertial subrange but steepening at the higher frequencies, as do the STATE 1 data. A detailed intercomparison of the probe data is presented, followed by an absolute comparison between the radar and rocket measurements. Reasonable agreement is seen between the observed echo power profile and the profile calculated using the 3-m electron density fluctuations obtained from the rocket data.

1. Introduction

The use of coherent backscatter radars has been recognized as an important way to monitor atmospheric conditions. In the troposphere and lower stratosphere, the radar backscatter signal depends upon aerosols and water vapor. In the mesosphere, the radar signature depends upon irregularities in the electron concentration. Major efforts have been made in the Federal Republic of Germany and in the United States to measure the properties of the mesosphere using coherent backscatter radar at VHF wavelengths. Since the Mesospheric, Stratospheric and Tropospheric (MST) radar at Poker Flat Research Range, Alaska (PFRR), is so well situated to allow comparison between rocket-borne sensors and the radar the Structure and Atmospheric Turbulence Environment (STATE) experiment [*Philbrick et al.*, 1984] was conducted there during the first 2 weeks of June 1983. In situ measurements of the atmospheric properties were made to compare to the MST radar signals in an effort to interpret the dynamical conditions in the middle atmosphere. The measurements were made during the summer season at PFRR, based on the large signals which have been measured by the MST radar over the past several years. Rockets with probes which can measure the electron irregularities with high spatial resolution were launched on three occasions which corresponded to selected conditions observed in real time in the radar data. In one of these cases, several other instruments were launched to study the structure of the neutral atmosphere. Profiles of density, temperature, wind and turbulence properties were measured. This paper and the three following ones are concerned with the results of the STATE campaign.

In this paper, electron density structure in the cold, polar summer mesosphere is investigated using rocket probes and MST radar data obtained at Poker Flat, Alaska, during STATE. The observed structure is believed to be the result of turbulence in the neutral atmosphere. A companion paper by *Kelley and Ulwick* [this issue], uses the rocket probe data to further investigate mesospheric structure and turbulence, a paper by *Watkins et al.* [this issue] utilizes the MST radar data to investigate turbulent energy dissipation rates and inner scale sizes, and a paper by *Fritts et al.* [this issue] examines the structure and characteristics of the gravity field.

As part of the STATE campaign, in situ high-resolution electron density probe measurements were made by rocket-
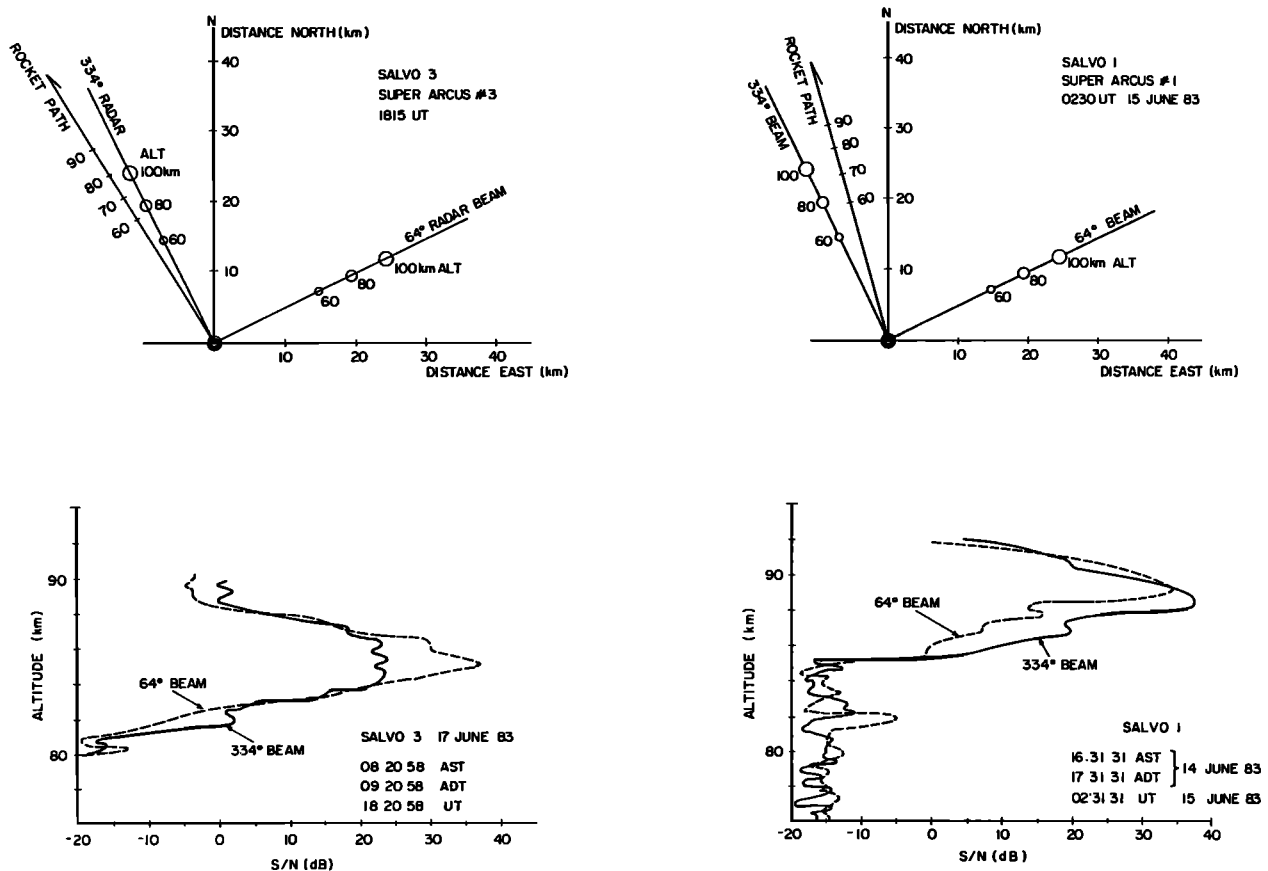
Fig. 1.   Poker Flat MST radar returns during the STATE rocket flights: salvo 1 (lower right panel) and salvo 3 (lower left panel). The upper panels show the radar beam azimuths and the rocket flight path for each case. The open circles on the radar beam line indicate the position and size of the radar scattering area, corresponding to the rocket altitudes. The radar signal-to-noise ratio (S/N) is in decibels.

borne dc probes on two Super Arcas rockets during salvos 1 and 3. The vertical spatial structure of mesospheric electron density fluctuations were obtained with spatial resolution down to about 10 cm. At mesospheric altitudes it is assumed that the motion of the electrons and ions is controlled by that of the neutral gas, owing to the high collisional frequency. The fluctuations in the profile can thus be used to derive the spectral scales of the turbulent motion [*Thrane and Grandel*, [1981]. Moreover, the electron density fluctuations should be directly related to the MST radar backscatter measurements, provided that the scattering arises solely from turbulent processes [*Balsley and Gage*, 1980]. In situ probe measurements are capable of measuring the overall spatial spectrum of the turbulent structure, while the radar is only sensitive to scales of one-half the wavelength of the electromagnetic wave, i.e., about 3 m. The electron density results from rocket salvos 1 and 3 and the corresponding MST radar measurements are the subjects of this paper.

The rocket probes consisted of simple dc probes (Langmuir type) flown on Super Arcas meteorological type rockets from the Poker Flat Research Range in Alaska during mid-June of 1983. The rockets achieved altitudes of about 100 km along azimuths near the "north" beam of the MST radar, also located at Poker Flat. The relative electron density was measured by monitoring dc electron current to the isolated tip (4.4-cm. length) of the nose cone, which was held at a fixed + 3-V bias potential with respect to the rocket skin. The paint

was removed from the rocket motors in order to provide a large area for the return positive ion current. The signals from the dc probe and a spin magnetometer were transmitted in a digital PCM format that used 16 bits per word and 16 words per frame, with a total rate of 8000 words s^{-1}. Thus the dc probe provided very high resolution measurements of the electron current, which is presumed to be approximately proportional to the electron density. Since no absolute electron density measurements were made on these payloads, a conversion factor was required to convert the magnitudes of the electron current to electron density values. A more recent Super Arcas rocket was flown that contained a dc probe identical to the STATE probes but additionally included an RF admittance probe for measurement of absolute electron densities. Since this rocket was geometrically and operationally identical to the STATE rockets and flew under similar conditions, i.e., at Poker Flat in the summer with similar solar zenith angle, we used these results to calibrate the STATE probes to obtain electron density values from the measured probe currents.

The Poker Flat 50-MHz MST radar consists of a large dipole antenna array driven by distributed transmitter modules [*Balsley et al.*, 1980]. The three fixed antenna beams were directed (1) in the vertical, (2) 15° off zenith on azimuth 64° geographic, and (3) 15° off vertical on azimith 334° geographic. Figure 1 shows the flight paths for the STATE 1 and 3 rockets relative to the antenna beam directions. Rocket posi-
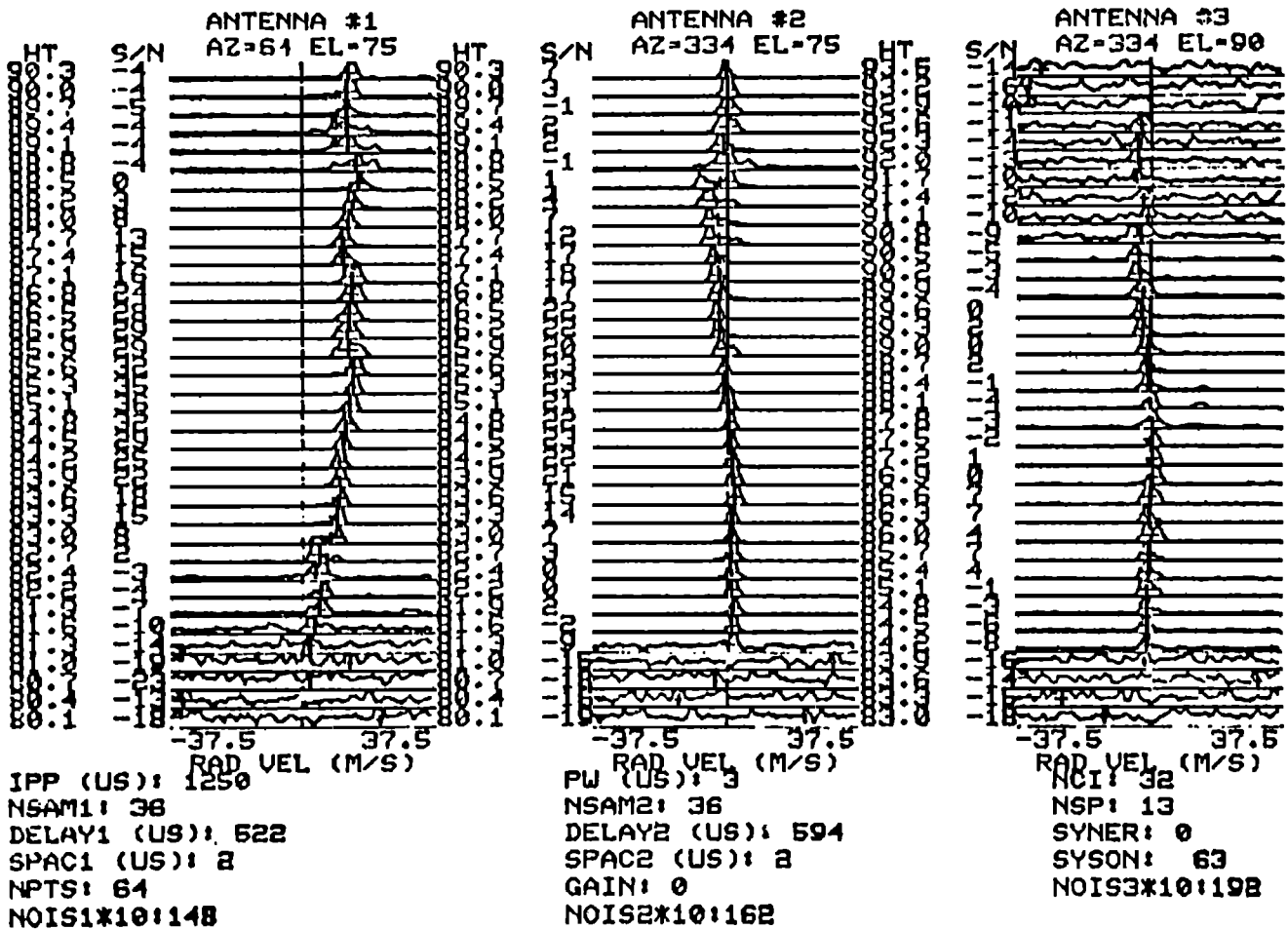
Fig. 2. Sample of the real-time display from the MST radar during the STATE Campaign. The radar signal-to-noise ratio (S/N) in decibels is plotted versus the indicated plasma radial velocity in meters per second for each of the three radar beams at various altitudes.

tion relative to the antenna beams for altitudes 60, 70, 80, and 90 km are shown for both launches. For both oblique beams the positions at the 60-, 80-, and 100-km regions of back-scatter are shown, with the diameter of the circles indicating the approximate areas of backscatter. Figure 1 shows that in both flights the rockets were less than 10 km away from the regions probed by the radar over the altitudes of prime interest (80–90 km).

In earlier studies the Poker Flat MST radar has typically been operated with a 15-μs pulse length in order to cover the tropospheric, stratospheric, and mesospheric scatter regions. This pulse length gives an altitude resolution of 2.2 km. For the STATE campaign, however, the radar data-gathering procedures were modified to allow the radar to accumulate data in 70 range bins on all three directions, where the resolution could be set between 300 m (2 μs) and 2.2 km (15 μs). It was thus possible to record data with 300-m altitude resolution over a continuous mesospheric height range between 70–100 km. Figure 2 shows a real time Doppler spectra recorded for each of the three antennas during a period of intense echo returns during the STATE campaign. This real-time capability of displaying the returned signals allowed optimization of the launch time of the rockets.

In the next section we describe the data analysis methods employed on the probe results in some detail and then give the results from the STATE 1 and STATE 3 rocket flights. A detailed intercomparison of the probe data is presented, followed by a comparison between the radar and rocket measurements. In a companion paper [Kelley and Ulwick, this issue] some additional implications of the joint data set are further discussed.

2. DATA PRESENTATION

2.1. Overview

The first rocket (STATE 1) was launched on June 15, 1983, at 0230 UT (1730 ADT) and the STATE 3 rocket was launched June 17, 1983, at 1820:58 UT, during periods of strong echo returns. The rockets reached peak altitudes near 100 km, with the rocket velocity changing from about 800 m s^{-1} at 70 km to about 450 m s^{-1} at 90 km. With a sampling rate of about 8000 Hz, this means that the spatial distance between sampling points changed from about 0.1 to 0.05 m over this height interval. Thus the spatial structure in the electron density could be determined well below the 3-m scale to which the radar is sensitive. Figure 3 shows the height profiles of the electron density (lower scale) and the MST radar echo signal-to-noise ratio (S/N) in decibels (upper scale) for both flights. It is obvious that in general, the large changes and strong gradients in electron density occurred in the re-
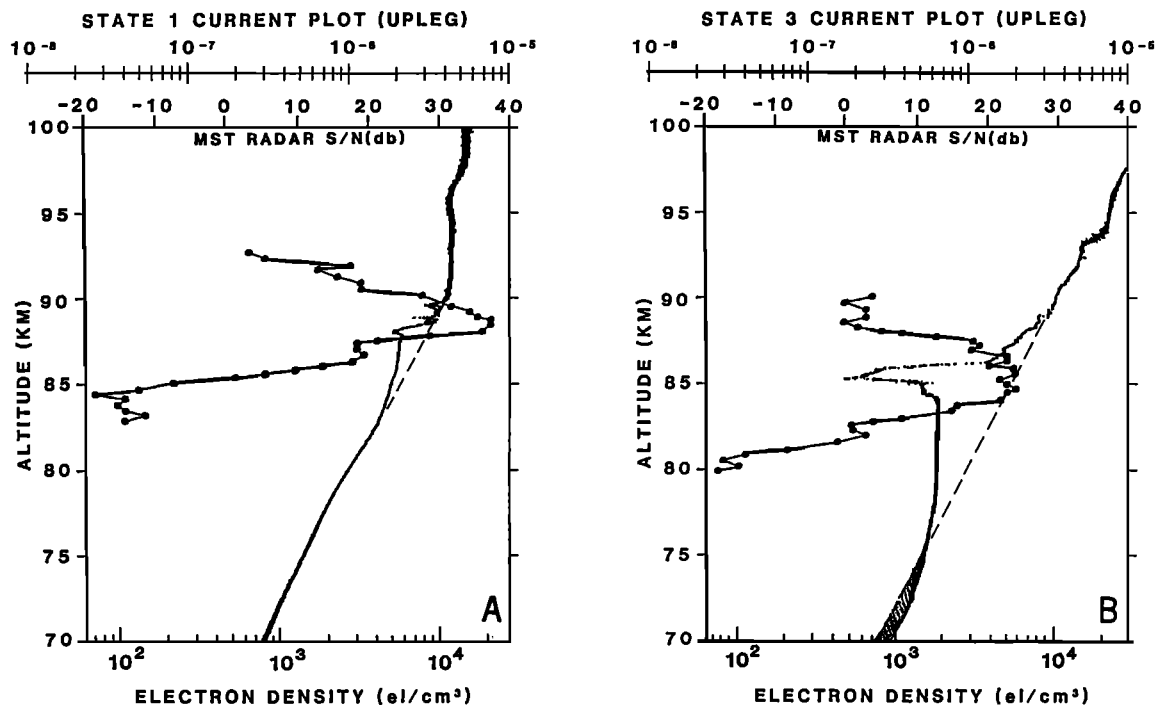
Fig. 3. Height profiles of the rocketborne dc probe results and MST radar echo S/N (solid circles) for the (a) STATE 1 and (b) STATE 3 rocket flights. The dc probe results are given both in (top scale) probe current and (bottom scale) tentative electron density values, assuming a constant proportionality between the two (see text). The dashed lines illustrate a more typical D region profile.

gions of most intense radar backscatter. It should be noted that the STATE 1 S/N peak in the radar data is about 37 dB near 88 km, whereas the STATE 3 S/N is much weaker and lower, reaching a peak of only 23 dB near 85 km. The STATE 3 results suggest that the region of radar backscatter corresponds to the altitude of steep gradients in the electron density caused by a deep "bite-out" in the electron density of almost an order of magnitude at 86 km. For STATE 1, however, the rapidly changing structure in the electron density and the corresponding sharp rise in the radar return power occur above the small depletion (about 10%) in the electron density profile near 88 km. Note that both electron density profiles are not typical of the normal D region. The STATE 3 profile is particularly atypical in that the vertical electron density gradient is almost zero from 77 to 84 km. (The dashed lines in Figures 3a and 3b emphasize this).

A power spectral analysis of the probe data was performed following the method of Blackman and Tukey [1958]. Spatial power spectra of the relative electron density fluctuations were first calculated from 2048 data points, corresponding to a time series of about 0.25 s to a height resolution better than 150 m in the altitudes of prime interest. This time series allowed the data to be spectrally analyzed in a frequency range extending to over 4000 Hz (i.e., a spatial resolution corresponding to scale sizes of about 12 cm). This resolution is considerably finer than the 3-m structure to which the 50-MHz radar is sensitive. In addition, longer time series were analyzed, using 2048 data points over 0.5-, 1.0-, 2.0-, 4.0-, and 8.0-s intervals, to examine the spectra at the lower frequencies (longer scale sizes). During these measurements the rocket spin rate was near 22 revolutions s^{-1}. Under these conditions, even tip-mounted probes suffer from some contamination at the spin frequency which is visible in the power spectra, if the data are

treated as is usually done by constructing deviations from a running mean. Since the spin effects were so prominent in the data, an attempt was made to remove these as much as possible by detrending the data, using a 12-term polynomial fit to the data. Power spectral analysis was conducted on both rocket data sets, and these will be discussed individually in the following paragraphs and then compared both with the radar data and with each other.

2.2. STATE 1

Inspection of the STATE 1 electron density results and the radar data in Figure 3 suggests that the power spectral analysis should be done in two time/altitude intervals: (1) from 95 to 111 s (76–85.8 km), where there were no strong radar echoes, and (2) from 111 to 123 s (85.5–92 km), where there were significant radar echoes.

2.2.1. Interval from 95–111 s (76–85.8 km). These data were spectrally analyzed in two time intervals, as shown in Figure 4a. No turbulent structure is apparent in the electron current measurements shown in interval 1, which is dominated by rocket spin effects. The power spectrum of these data, shown in Figure 4b, shows the only significant spectral component to be at the spin frequency (approximately 22 Hz). Interval 2 of Figure 4a exhibits more structure in the current data, and the corresponding spectrum in Figure 4c shows a distinct increase in fluctuation power at frequencies below 100 Hz. It should be noted in Figure 4c that the noise level at high frequencies decreased with increasing altitude compared with Figure 4b, an effect which was also observed by Royrvik and Smith [1984] in their investigation of mesospheric turbulence in Peru.

In power spectral analysis it is sometimes useful to fit a power law to the spectrum to determine the spectral index n,
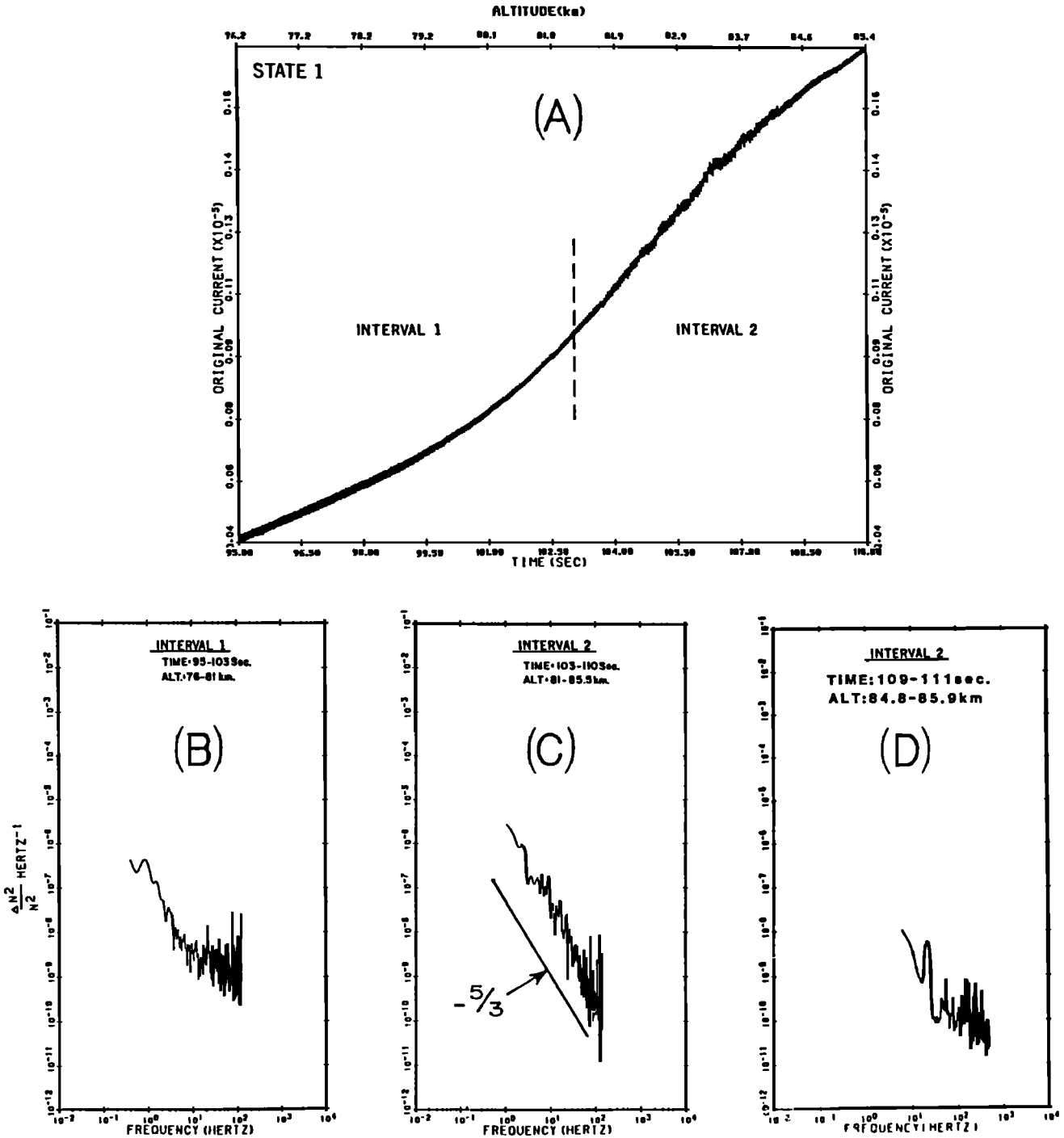
Fig. 4. The dc probe results for the STATE 1 rocket: (a) probe current versus time; (b) interval 1, 95–100 s; and (c) interval 2, 103–110 s; and (d) interval 2, 109–111 s, the power spectral analysis of the fluctuations.

using the relationship $P(\omega) \propto \omega^n$. For a probe traveling at a high velocity, V_R, with respect to the irregularities, this is equivalent to a one-dimensional spectrum $S(k) \propto k^n$, where $k = \omega/V_R = 2\pi/\lambda$. The spectral index for Figure 4c between 1 and 100 Hz was found to be about -1.7; a value reasonably close to the $-(5/3)$ value predicted by turbulent theory for a one-dimensional spectrum of density fluctuations in an inertial subrange of homogeneous, isotropic turbulence [*Tartarskii*, 1961]. With a rocket velocity of about 500 m s^{-1} in this time interval, Figure 4c suggests that the inertial subrange of turbu-

lence extends at least over the range from 500 down to about 10 m (where the slope breaks).

Since the current probe signal is rather weak in this height interval, we cannot resolve the 165-Hz portion of the spectrum (i.e., the frequency corresponding to the 3-m structure responsible for the radar echoes) as was done in subsequent time intervals. However, we certainly can say that the fluctuations were stronger in the 81- to 85-km range than in the 76- to 81-km range, based on the results shown in Figures 4b and 4c. This increase in fluctuation strength agrees with the radar
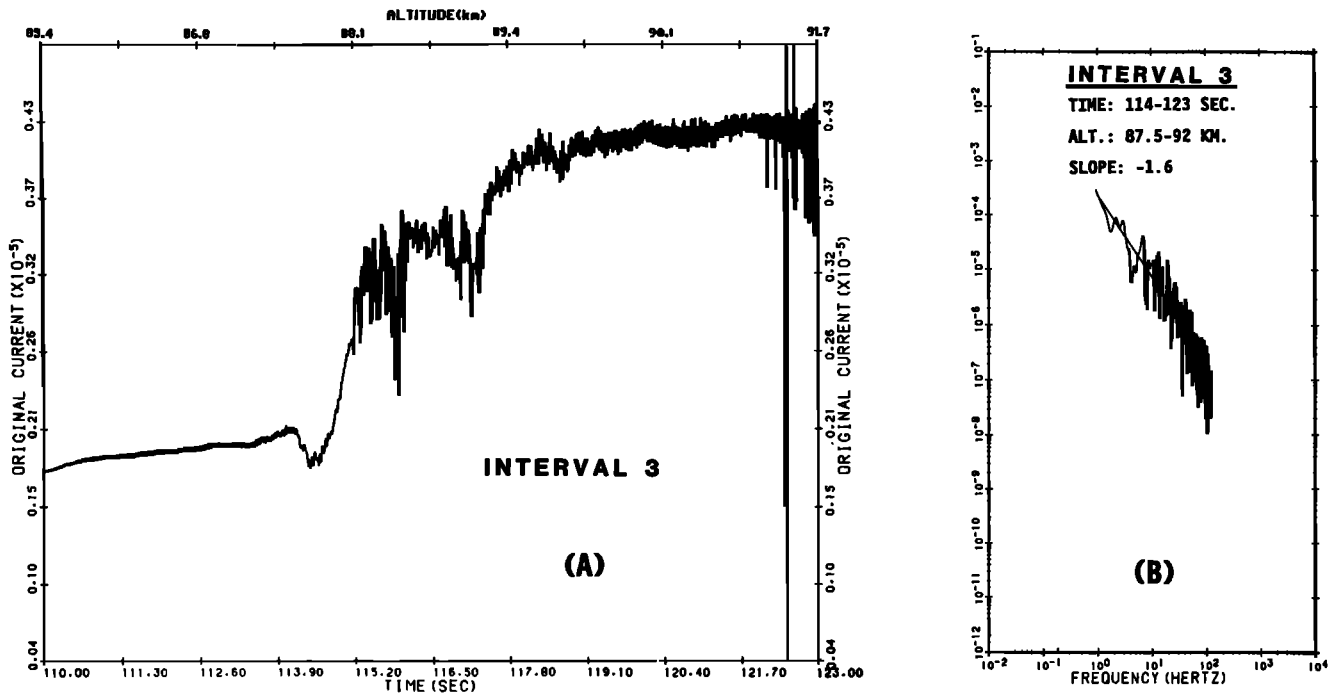
Fig. 5. (a) Profile shows the electron current and defines interval 3. (b) The power spectrum of the electron density fluctuations in the last 9 s of interval 3.

data, which also show an increase in signal power at 83 km relative to echoes below about 82.5 km (which were not detectable) and at the higher altitude at 84.5 km, as shown in Figure 3. To further study this weak relative maximum in the radar echoing power, we have concentrated on the 2-s interval from 109 to 111 s and plotted its power spectrum in Figure 4d. Indeed, the fluctuation signal is very weak over the whole frequency range, with the spike at the spin frequency of 22 Hz dominant. There is also a minimum in radar S/N near 84.5 km, as shown in Figure 3. Thus the rocket data are in reasonable agreement with the radar echo power over the height range from 81 to 84.5 km, even in this region of very weak radar signal (−10-dB S/N for the radar data).

2.2.2. *Interval from 111–123 s (85.5–92 km)*. The probe current collected during the 110- to 123-s time interval is shown in Figure 5a, using a current scale about one-third that in Figure 4 because of the much larger variations in the current over this height interval. The spectra from 110 to 114 s (not shown) are very similar to those of Figure 4c, i.e., the signal is rather weak at the 3-m wavelength of the radar but shows a distinct power increase at frequencies below 100 Hz. Analysis of the data between 111–123 s at 0.5-s intervals (to be discussed later) shows that significant power increases at frequencies corresponding to 3-m wavelengths began at a rocket altitude of 86.6 km. The MST radar showed a rapid increase in the echo return power, beginning at about 84.7 km (about −15 dB S/N) and increasing to a value near 17 dB at 86.6 km, where the rocket probe data at 3 m shows significant power increases. Thus it is obvious that the MST radar exhibits much more sensitivity to the 3-m structure than does the probe data. Still, it is very encouraging that both techniques detect the two regions with turbulent structure (81–84.5 km and above 86.6 km) and the region of little or no detectable turbulence separating them. Detailed comparison of the rocket and radar results is presented in section 3.2 of this paper.

To study the region from 114 to 123 s (Figure 5a), we first analyze the whole interval, as shown in the spectrum in Figure 5b. Comparing Figure 5b with Figures 4c and 4d, the fluctuation power is higher by 2–4 orders of magnitude. This very strong signal allows us to perform a detailed study of the spectra in this height range. Two aspects are immediately clear: at the lower frequencies (small k values), the spectral index is near −1.6; however, as k increases, the spectrum becomes much steeper. These characteristics are exactly as one would predict for a passive scalar mixed by a turbulent neutral fluid, since theory for such a process predicts that the one dimensional spectrum of a passive scalar should display a −(5/3) slope in the inertial subrange, with a break to a steep slope occurring at some large value of k [*Driscoll and Kennedy*, 1985]. A detailed discussion of the mixing physics as implied by the present data set is reserved for a companion paper [*Kelley and Ulwick*, this issue].

To examine the spectral characteristics in more detail, the data from 115 to 123 s were analyzed over four 2-s intervals. The spectra in Figure 6 clearly change from forms characteristic of mesospheric turbulence (Figures 6a and 6b), to the "white noise" power spectrum in Figure 6d, which is almost certainly due to plasma instabilities in the lower E region [*Fejer and Kelley*, 1980]. It is well known that such structures do not scatter 50-MHz radar signals transmitted at high elevations in the polar regions, since the plasma waves are such that $k * B = 0$, i.e., they produce highly anisotropic scattering with a maximum scattering cross section perpendicular to the Earth's magnetic field. The steep spectral index for higher frequencies is clearly shown in Figures 6a and 6b. In Figure 6a the power law spectral index of −1.6 from the results of Figure 5b has been superimposed on the spectrum. In the higher frequency range, a power law with index −7.0 is also shown.

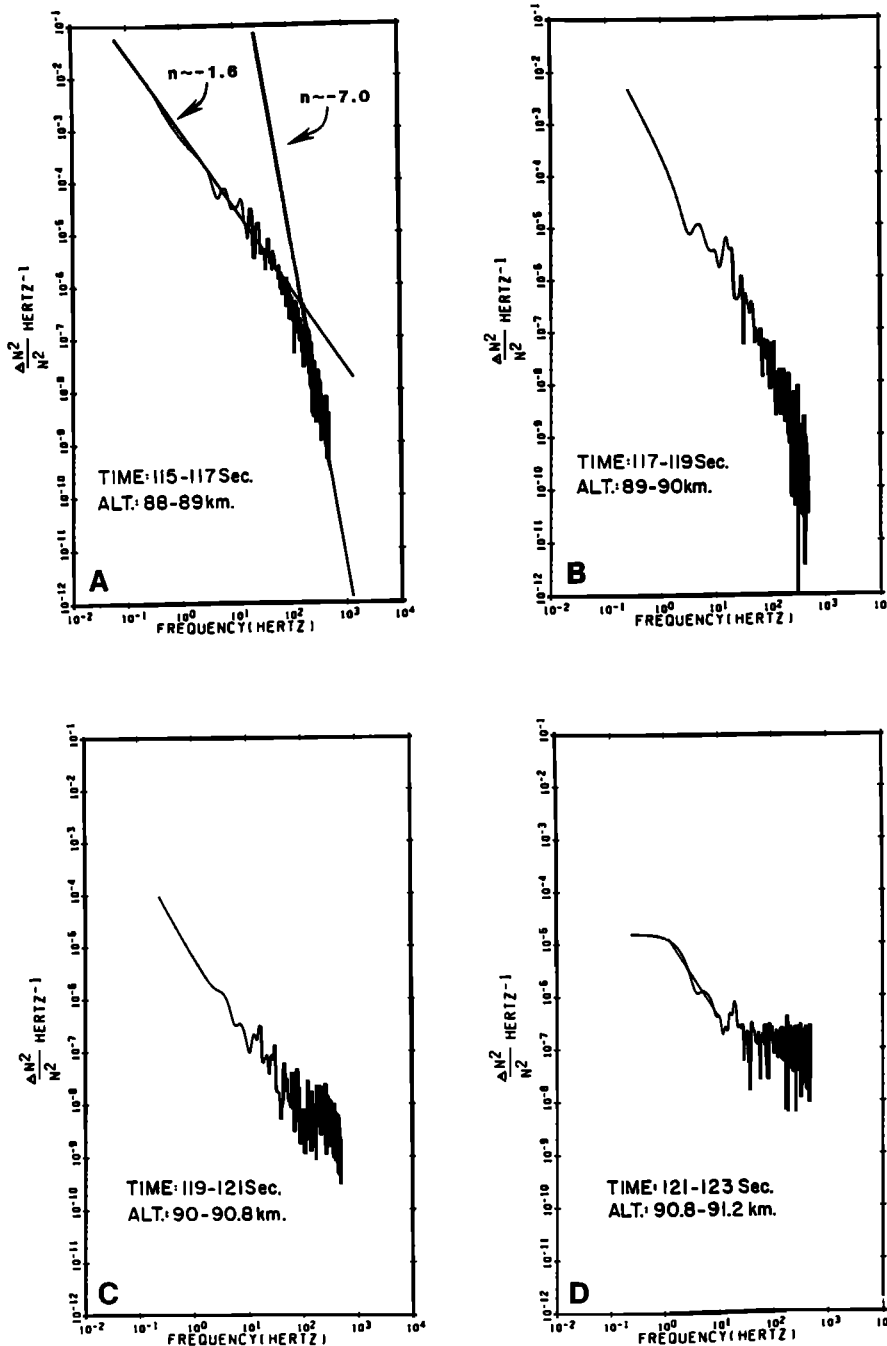Figure 7 shows a composite power spectrum covering the

Fig. 6.   STATE 1 electron density power spectral analysis results for 2-s intervals between 115 and 123 s: (a) 115–117 s; (b) 117–119 s; (c) 119–121 s; and (d) 121–123 s.

time period from 114 to 118 s (the region showing the largest current fluctuations). For the lower frequencies between 1 and 100 Hz (corresponding to wavelengths of about 550–5.5 m), the entire time period was used. At the higher frequencies between 10 and 1000 Hz (corresponding to wavelengths of 55 to 0.5 m), the spectrum was obtained by averaging all 0.25-s spectra in the time interval 114–118 s. The two plots are superimposed and overlaid in the 10- to 100-Hz range. Additional scales of wavelength (in meters), $[\Delta N/N]^2/Hz^{-1}$, and wave number (in radians per meter) are also included in the plot. Spectral indications of -1.6, -3.0, and -7.0 are shown to compare with the composite spectrum. Also shown is the 3-m MST radar operating frequency (about 165 Hz). The rise

in power at 10 Hz is caused by an interference due to an on-board magnetometer and should be ignored.

2.3. STATE 3

The electron density profile for STATE 3 shown in Figure 3 was analyzed in two intervals: from 100 to 110 s (62.8–82.9 km), and 110 to 120 s (82.9–87.8 km), as shown in Figure 8. The short time interval spectra from 80 to 110 s were all very similar, with spin effects dominating, as can be seen in Figure 8a. Essentially no evidence for turbulence was found in this range. For example, Figure 8a shows the spectrum for 77.2–82.9 km, which has a strong peak between 20 and 30 Hz. In contrast, the spectrum from 82.9 to 87.8 km (Figure 8b) has
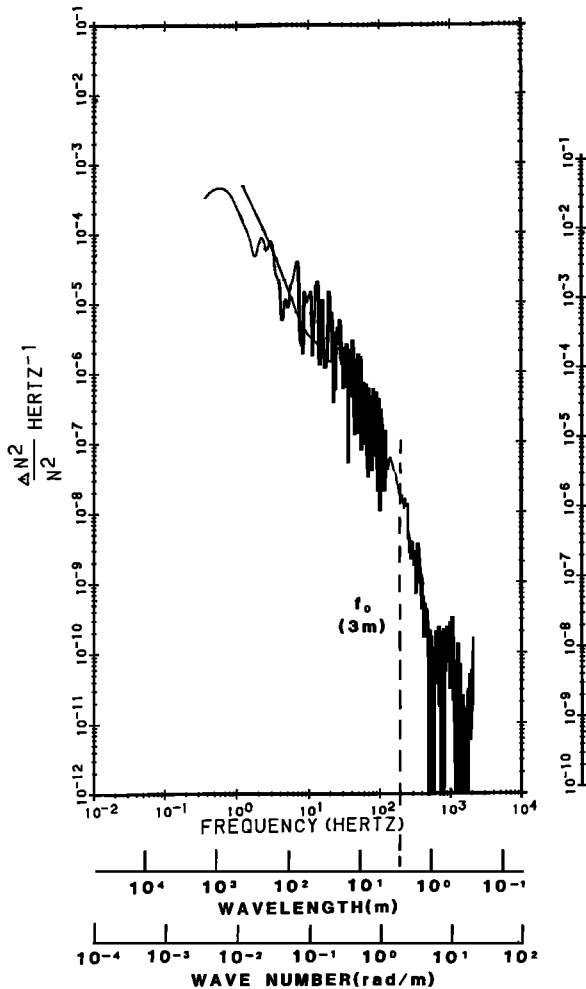
Fig. 7. Composite power spectrum from STATE 1 results for the interval from 114 to 118 s (see text).

very high power levels. The spectral index of a straight-line fit is about -1.8 from 1.0 to 50 Hz in Figure 8b, and the fluctuation power is up by about 2 orders of magnitude in comparison with the plot in Figure 8a for the same frequency range. As noted earlier, the intense radar backscatter signal is centered in the region of the "bite-out" of the electron density profile, as is the spectrum plotted in Figure 8b.

In Figure 9a the averaged spectrum for all 0.5-s spectra in the 110- to 120-s (82.9–87.8 km) interval is superimposed on the spectrum from Figure 8b. In Figure 9b the composite spectrum (Figure 7), obtained in the same way as for STATE 1 (87.5–89.5 km), is repeated for comparison. (The background noise level at high frequencies is near 10^{-10} Hz^{-1} for both flights).

3. DISCUSSION

3.1. Comparison of STATE 1 and STATE 3 Results

Although only a few days separated the two rocket flights, the relationship between the electron density profile and the radar scattering profile is quite different for the two measurements. In STATE 3 a broad depletion in electron density seemed to commence at about 75 km. Between 77 and 84 km,

instead of the usual monotonic increasing profile, there was almost no vertical density gradient at all. At 85 km the density abruptly began to decrease, resulting in a net depletion of nearly an order of magnitude when compared with a more normal profile. The radar scattering region was exactly centered on this deep "bite-out" in the electron density. This depletion occurred within the broad temperature minimum (80–92 km), detected on June 15, 1983 (C. R. Philbrick, private communication, 1986). *Johannessen and Krankowsky* [1972] reported a very similar ionization profile (i.e., a sharp ledge near 85 km, a sharp minimum immediately below the ledge, and a depletion width of about 1 km) from a probe on a rocket launched to study the ion composition of the cold summer, northern-latitude mesopause. Although we cannot be entirely sure at this time, we speculate that this region of depeleted electron density is due to the attachment of electrons to hydrated molecules associated with polar mesospheric clouds. The resulting heavy negative ions would not be collected as efficiently by the Langmuir probe, whose response reflects the electron content of the gas.

The resulting sharp gradients in electron density then may be mixed by turbulent atmospheric motion in this mesopause region and may lead to the strong backscatter echoes. This contention is supported by the presentation in Figure 10, where the electron density (N_e) profile is plotted again along with the high-resolution spectral information $(\Delta N_e/N_e)^2 N_e^2$. For this plot we have integrated the 0.5-s density fluctuation spectra in the $0.75 k_0 \leq k < 1.25 k_0$ range, where k_0 is the radar scattering wave number. Three defined peaks at about 84.5, 85.2, and 86.1 km are identified by arrows as 1, 2, and 3. These peaks are coaligned, with clearly visible structure imbedded in the sharp electron density gradients. The electron density is varying as much as 40% within the structures, and the more the variability, the higher $\Delta N_e^2(k_0)$. (Note that $\Delta N_e^2(k_0) = (\Delta N_e/N_e)^2$ H$^{-1} \times N_e^2$ cm^{-1}). Conversely, when there is significantly less structure in N_e, e.g., between 1 and 2 and 2 and 3, $\Delta N_e^2(k_0)$ is much lower. As pointed out by *Thrane and Grandel* [1981] and others, the efficiency of electron structuring driven by neutral turbulence is directly proportional to the electron density gradient scale length, $L = [1/n(dn/dz)]^{-1}$. On the upper edge of this bite-out, L is less than approximately 200 m, which is very steep indeed. Further discussion of this structuring process is given by *Kelley and Ulwick* [this issue].

Turning to the STATE 1 data in Figure 3, there is also weak evidence for a large-scale depletion in the profile, but no deep bite-out. The radar echoes and the in situ structure measurements both show a first indication of activity near 86 km (shown in section 3.2.), the same altitude at which the bite-out occurred during STATE 3 and very near the minimum in the atmospheric temperature measured on June 15, 1983. To first order, the radar echoes and the in situ turbulence maximize on the steepest part of the upward electron density gradient between 87.5 and 90 km. The STATE 1 gradient is much weaker than the STATE 3 gradients, with $L \simeq 4$ km.

In Figure 11 we compare the rocket ascent and descent results from STATE 1. The rocket on descent at 88 km was about 25 km northwest of the ascent position at the same altitude. Clearly, the electron density is structured near the same altitude (within the uncertainties of the rocket trajectory), but the characteristics of the turbulence are quite different. This perhaps is not surprising, since the radar results indicate spatial variations of the structured regions (e.g., see
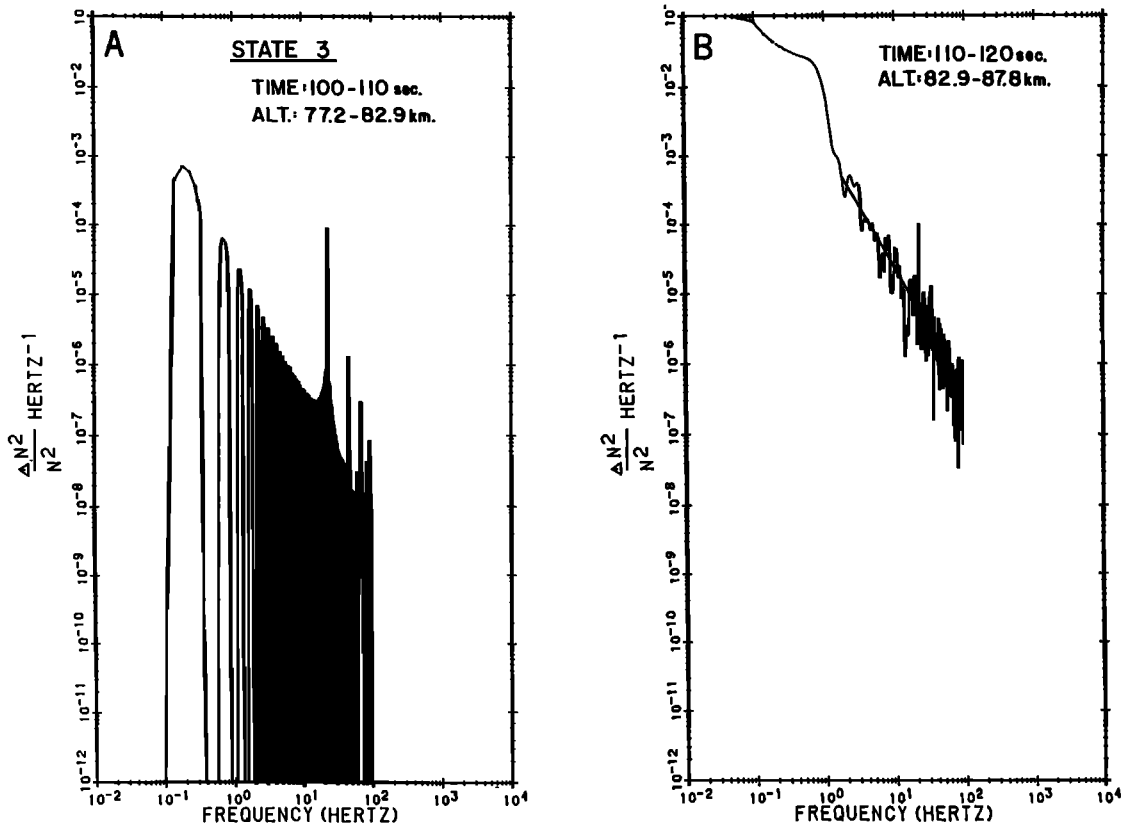
Fig. 8. Power spectral analysis of electron density fluctuations from the STATE 3 rocket: (a) 100–110 s and (b) 110–120 s.

Figure 3). Note, however, that above the depletion in both profiles near 88 km, the descent results show a deep bite-out more similar to the STATE 3 results, i.e., steep gradients, large electron density bite-out, and structure imbedded in the gradients. The descent data are complicated by a spin/coning effect near and after apogee, characteristic of very lightweight Super Arcas rocket payloads, making spectral analysis difficult.

An expanded zero-order electron density profile and the $\Delta N_e^2(k_0)$ parameter discussed earlier are plotted for STATE 1 in Figure 12 for rocket ascent. This presentation seems to show a fine structure on the zero-order electron density gradient, which, in turn, organizes the fine-scale structure of the turbulence. For example, the relative minima in local electron density at 87.7, 88.4, 89.2, and even at 89.8 km, all show relative maxima in the turbulent power at small scales. This feature is discussed further by Kelley and Ulwick [this issue], who speculate that the large-scale wave process responsible for the turbulence in the neutral atmosphere above the mesopause has a vertical structure which organizes the local regions of intense small-scale (e.g., 3 m) turbulence.

Turning now to a comparison of the spectral data in Figure 9, both data sets show a change in spectral slope around 100 Hz. The difference in slope is much more pronounced in STATE 1 than in STATE 3. The STATE 1 data appear much more like a classical passive scalar mixed by turbulence, both in spectral form and by visual inspection, than do the STATE 3 data. As discussed in more detail by Kelley and Ulwick [this issue], this may be the consequence of a significant contribution to the STATE 3 spectrum by the very steep edges on the electron density profile. Such an edge tends to introduce a

k^{-2} dependence in a power spectrum and could contribute to the steeper k spectrum at small k.

If the two $(\Delta N_e/N_e)^2$ spectra are overlaid and the power levels made to match at 100 Hz, the spectral shape is nearly identical for $f \geq 100$ Hz. This suggests that the process which leads to a steep spectrum, e.g., diffusive damping, is nearly identical for the turbulence-driven case (STATE 1) and edge-steepened plus turbulence-driven case (STATE 3).

Finally, at the frequency and wave number corresponding to 3-m waves, the STATE 3 $(\Delta N_e/N_e)^2$ power is roughly a factor 2 higher than the power detected during STATE 1. This at first glance seems to be a paradox, since the radar scattering is some 16 dB stronger for STATE 1. However, the radar scattering power is proportional to $(\Delta N_e/N_e)N_e^2$, not just $(\Delta N_e/N_e)^2$, and N_e^2 is roughly 64 times greater in the STATE 1 case. The net predicted increase in radar power is thus roughly a factor of 32, which corresponds to 15 dB. This relative comparison is very encouraging. In the next section a detailed quantitative calculation of the expected scattering power is made.

3.2. Rocket and Radar Comparison

In order to examine the relationship between the electron density fluctuations and the MST radar signal-to-noise ratio, the pulsed-radar equation for volume-filled scattering presented by Balsley and Gage [1980] can be expressed as

$$\sigma = \frac{2\pi c k_B (T_s + \alpha T_C)}{P_T A_e \alpha^2 F_i} \left(\frac{r}{\Delta_r}\right)^2 \frac{S}{N} \tag{1}$$
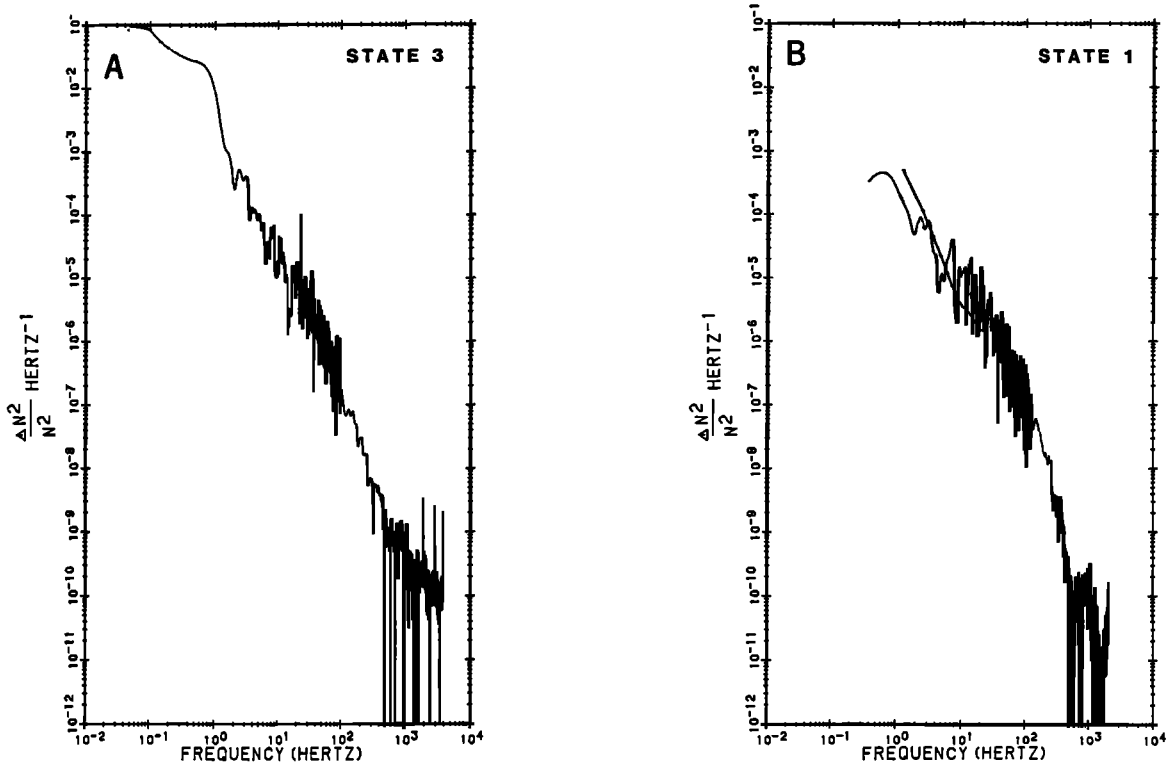
Fig. 9. (a) Average of 0.5-s power spectra from the STATE 3 rocket in the interval from 110 to 120 s. (b) Similar data from the STATE 1 rocket, repeated here for comparison.
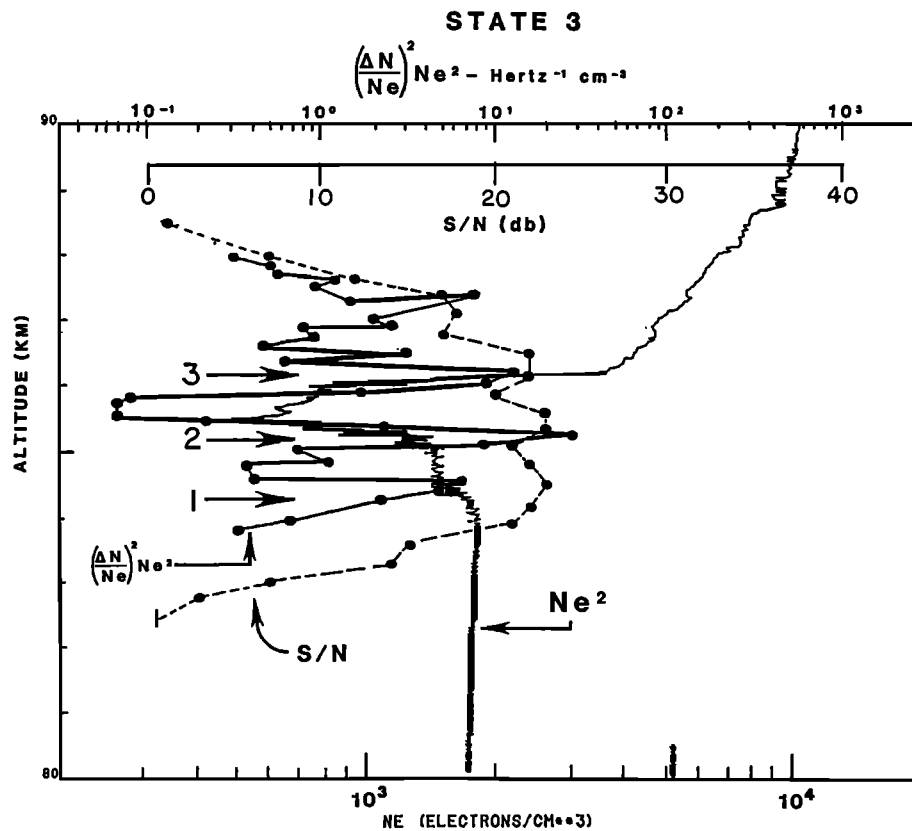

Fig. 10. High-resolution power spectra of electron density fluctuations, plotted along with the electron density profile for the STATE 3 results.
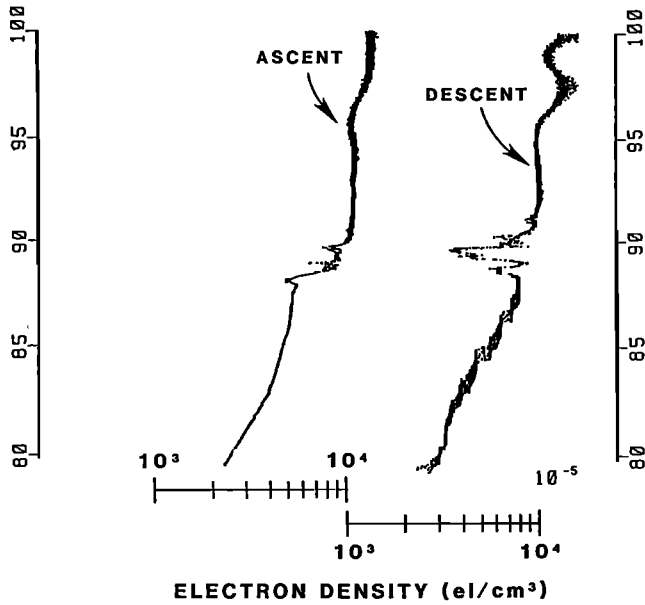
Fig. 11. Rocket ascent and descent electron density profiles from the dc probe on STATE 1 rocket.

where c is the velocity of light and k_B is the Boltzmann's constant. The definitions and values of the Poker Flat radar parameters are given in Table 1.

Equation (1) reduces to

$$\sigma = 1.15 \times 10^{-17} \, S/N \, m^{-1} \tag{2}$$

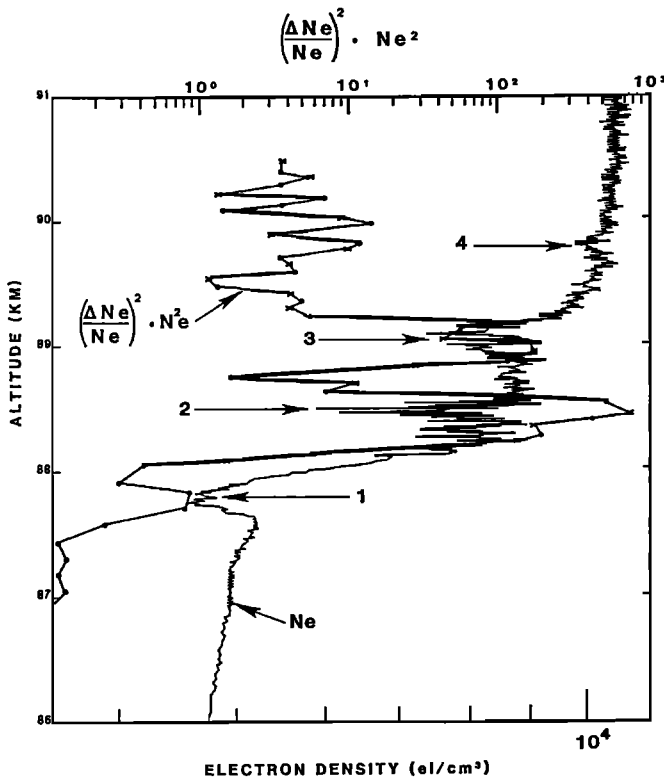*Royrvik and Smith* [1984] derived the reflectivity in terms of

Fig. 12. Expanded zero-order electron density profile (dots) and N_e^2 parameter (crosses) (see text). Arrows indicate altitudes of relative minima in electron density and maxima in turbulent power at small scales.

TABLE 1. MST Radar Parameters

Symbol	Definition	Value
σ	radar volume reflectivity	$\cdots$
S/N	spectral total signal-to-total noise ratio	$\cdots$
r	range	88.49×10^3 m
Δr	range resolution	300 m
T_s	system noise temperature	400°K
T_c	cosmic noise temperature	4000°K
α	resistive antenna losses	0.65
A_e	effective antenna area	3×10^4 m^2
P_T	peak transmitted power	1.46×10^6 W
F_i	number of coherent integrations	32

the rocket irregularity spectrum, to obtain

$$\sigma(k) = -n\left(\frac{\pi}{8}\right)k^2 \frac{f_p^4}{4f^4}\left[\frac{S_n(k)}{N_e^2}\right] \tag{3}$$

where n is the spectral index; k, 2.1 rad m^{-1}, f_p, the plasma frequency; f, the frequency of the probing wave; $S_n(k)$, the one-dimensional spectrum measured by the rocket (in meters per radian); and N_e, the electron density (in cubic meters). Equation (3) reduces to

$$\sigma(k) = 4.5 \times 10^{-28}(-n)N_e^2 \left[\frac{S_n(k)}{N_e^2}\right] \tag{4}$$

combining (4) and (2)

$$S/N = 3.91 \times 10^{-11}(-n)N_e^2 \left(\frac{S_n(k)}{N_e^2}\right) \tag{5}$$

Finally, in order to compute S/N using the existing data analysis, which is expressed in units of $(\Delta N_e/N_e)^2$ Hz^{-1}, (5) is rewritten as

$$S/N = \frac{3.91 \times 10^{-11}(-n)N_e^2 V_R}{2\pi}\left(\frac{\Delta N_e}{N_e}\right)^2 \tag{6}$$

where V_R is the rocket velocity in meters per second. These expressions are valid provided the electron density fluctuations are isotropic and have a negative power law scale size distribution.

The calculated S/N from (6) at 0.5-s intervals, corresponding to a height resolution of about 250 m (compared with the radar 300-m height resolution) is shown in Figure 13a for STATE 1, with the radar S/N measurement superimposed. The agreement in general is good, although the calculated values are noticeably higher at the peak S/N. The S/N from the rocket data is shown as 0 dB from about 84 to 86.4 km, because a spectral index could not be resolved. Above 90 km, no S/N could be calculated, since, as mentioned, the spectra above this altitude all have "white noise" characteristics more typical of plasma processes which are not isotropic and which do not scatter the radar signals at such high elevation angles (k must be perpendicular to B to receive scatter from such plasma waves).

In Figure 13b the signal-to-noise calculated using 0.5-s time series (250-m height resolution) spectra from STATE 3 rocket probe measurements shows much more structure than the radar S/N. The radar S/N for STATE 3, however, does show indications of structure and certainly shows more than the STATE 1 radar measurements. If a time series over 2-s intervals is used, considerable smoothing results, as shown in Figure 10b.
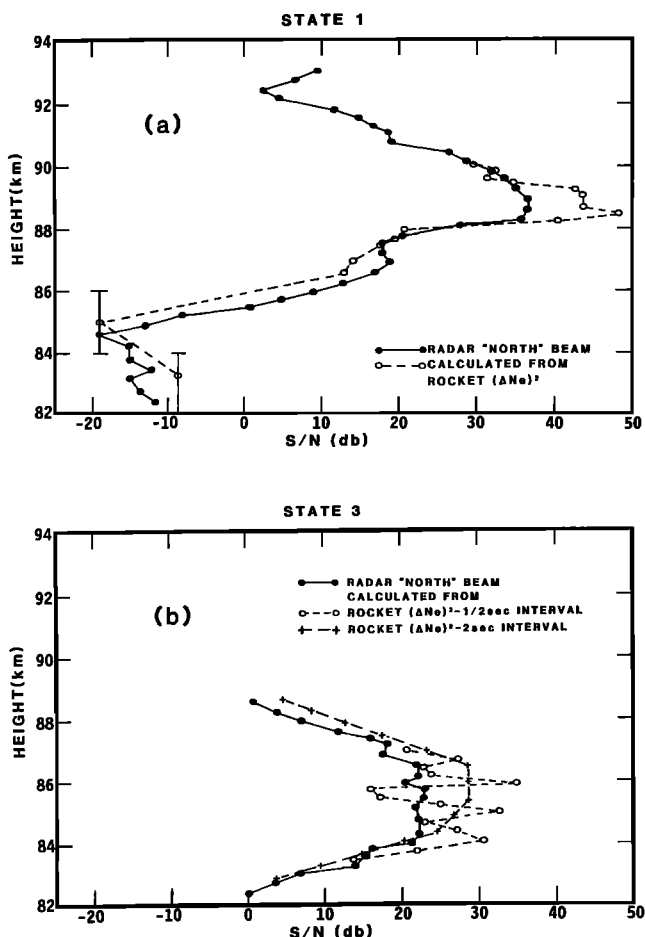
Fig. 13. MST radar echo power (S/N) measured by the north beam and calculated from the high-resolution electron density power fluctuations measured by the rocket probes: (a) STATE 1 results and (b) STATE 3 results.

4. SUMMARY

The data from the two Super Arcas rocket electron density probes during the STATE campaign, coupled with the MST radar data, have given very new and interesting results on the cold summer polar mesosphere, as contained in this paper and the companion paper by *Kelley and Ulwick* [this issue]. We summarize the main results from this paper as follows:

4.1. STATE 1

1. The altitude profile of the MST radar echo power is in excellent agreement with the structure in the electron density observed in the rocket data, even in regions of weak radar signal. The structured region is mostly on or above the steep gradient in electron density.

2. The power spectra characteristics are exactly as one would predict for a passive scalar mixed by a turbulent neutral fluid, although an anomously high Schmidt number is required [see *Kelley and Ulwick*, this issue].

3. The calculated signal-to-noise ratio from the one-dimensional spectra measured by the rocket is in good agreement with the MST radar S/N profile.

4. The structured region shows distinctive spatial variations.

4.2. STATE 3

1. The intense radar backscatter signal is centered on a deep "bite-out" in the electron density profile. The structured

region is mostly on or below the sharp gradient in electron density.

2. For frequencies less than 100 Hz, the spectral slope is influenced by the steep edges on the electron density profile.

3. The characteristics of the power spectra for frequencies greater than 100 Hz are identical to STATE 1, suggesting that the process leading to a steeper spectrum is nearly identical for the turbulence-driven case (STATE 1) and edge-steepened plus turbulence-driven case (STATE 3).

4. The radar S/N measurements appear to smooth the more structural S/N profile from the electron density measurements.

REFERENCES

Baker, K. D., J. LaBelle, R. F. Pfaff, L. C. Howlett, N. B. Rao, J. C. Ulwick and M. C. Kelley, Absolute electron density measurements in the equatorial ionosphere, *J. Atmos. Terr. Phys.*, 47, 781, 1985.

Balsley, B. B. and K. S. Gage, The MST radar technique: Potential for middle atmospheric studies, *Pure Appl. Geophys.*, 118, 452, 1980.

Balsley, B. B., W. L. Ecklund, D. A. Carter, and P. E. Johnson, The MST radar at Poker Flat, Alaska, *Radio Sci*, 15, 213, 1980.

Blackman, B. B., and J. W. Tukey, *The Measurement of Power Spectra*, Dover, New York, 1958.

Driscoll, R. J., and P. Kennedy, A model for the spectrum of passive scalars in an isotropic turbulent field, *Phys. Fluids*, 28(1), 72–1985.

Fejer, B. G., and M. C. Kelley, Ionospheric irregularities, *Rev. Geophys.*, 18, 401, 1980.

Fritts, D. C., S. A. Smith, B. B. Balsley and C. R. Philbrick, Evidence of gravity wave saturation and local turbulence production in the summer mesosphere and lower thermosphere during the STATE experiment, *J. Geophys. Res.*, this issue.

Johannessen, A., and D. Krankowsky, Positive-ion composition measurement in the upper mesosphere and lower thermosphere at a high latitude during summer, *J. Geophys. Res.*, 77, 2888, 1972.

Kelley, M. C., and J. C. Ulwick, Large- and small-scale organization of electrons in the high-latitude mesosphere: Implications of the STATE data, *J. Geophys. Res.*, this issue.

Philbrick, C. R., D. P. Sipler, B. B. Balsley, and J. C. Ulwick, The STATE experiment—Mesospheric dynamics, *Adv. Space Res.*, 4, 129–132, 1984.

Royrvik, O., and L. G. Smith, Comparison of mesospheric VHF radar echoes and rocket probe electron concentration measurements, *J. Geophys. Res.*, 89, 9014, 1984.

Tartarskii, V. I., *Wave Propagation in a Turbulent Medium*, McGraw-Hill, New York, 1961.

Thrane, E. V., and B. Grandel, Observations of fine scale structure in the mesosphere and lower thermosphere, *J. Atmos. Terr. Phys.*, 43, 179, 1981.

Watkins, B. J., C. R. Philbrick, and B. B. Balsley, Turbulence energy dissipation rates and inner scale sizes from rocket and radar data, *J. Geophys. Res.*, this issue.

K. D. Baker and J. C. Ulwick, Department of Electrical Engineering, Utah State University, Logan, UT 84322.

B. B. Balsley and W. L. Ecklund, Aeronomy Laboratory, National Oceanic and Atmospheric Administration, 325 Broadway, Boulder, CO 80303.

M. C. Kelley, School of Electrical Engineering, Cornell University, Phillips Hall, Ithaca, NY 14853.